AUTOMOTIVE RADAR APPLICATION FOR STRUCTURAL HEALTH MONITORING

ENNIO GAMBI, GIANLUCA CIATTAGLIA & ADELMO DE SANTIS
Department of Information Engineering, Polytechnic University of Marche, Italy

ABSTRACT

Monitoring of communication and residential infrastructures, such as buildings, bridges and tunnels, has always been important to ensure the safety of citizens. In particular, it is of interest to verify the level of mechanical stress to which bridges and buildings are subjected during earthquakes, measuring the oscillations that the structure undergoes during the seismic event, in order to verify the overcoming of safety thresholds, in which stability may be impaired. In this paper the mmWave radars designed for the automotive world is taken into account, since it allows high precision measurements at a relatively low cost. mmWave radars are able to detect vibrations of the order of tens of microns and, therefore, are very useful for monitoring buildings. Furthermore, using MIMO (Multiple Input Multiple Output) mmWave radars, it is possible to implement the Beamforming technology for the spatial shaping of the radio beam, in order to detect more targets simultaneously. In this way it is possible to monitor multiple buildings or structures simultaneously, or different parts of the same structure with a single sensor. The objective of the present work is to show the applicability of automotive radar to the measurement of oscillations suffered by buildings and bridges, in order to be used as a monitoring tool in the event of earthquakes. Results of software simulations, laboratory test and real measurements on infrastructures are provided.

Keywords: mmWave radar, contactless measurements, radar sensors.

1 INTRODUCTION

Recent events in Central Italy, such as the seismic events of 2016–2017 or the collapse of the Morandi Bridge of Genoa in 2018 have increased awareness on the importance of communication and residential infrastructures monitoring. In order to ensure the citizen safety, buildings, bridges and tunnels must be constantly monitored, implementing acquisition systems supervised by artificial intelligence algorithms in order to identify any anomalous or dangerous situations. In particular it is of interest to verify the level of mechanical stress to which bridges and buildings are subjected during earthquakes, measuring the oscillations that the structure undergoes during the seismic event, with the aim to verify the overcoming of safety thresholds, in correspondence of which stability may be impaired.

For this purpose, many technologies based on contact measurements are available, that may be implemented with accelerometers [1]. In some applications, however, it is necessary to monitor the behavior with non-contact or remote methods, such as the laser or radar methodologies that provide a measure of the oscillations suffered by the structures on the basis of the analysis of the signal reflected by the structure under examination. RADAR interferometry for non-contact measurements has been applied for some time now, usually using non-commercial and often customized designed systems. In [2], [3] a radar with Stepped-Frequency Continuous Wave (SF-CW) modulation is considered, while in [4] a Frequency-Modulated Continuous Wave (FMCW) radar is taken into account. In [5] a comparison between RADAR vibration and accelerometer measurements is reported. The comparison shows how these two sensors generate signals with the same oscillation frequencies even if with different amplitudes. However, the radar highlights motion components that the accelerometer is unable to detect.

WIT Transactions on The Built Environment, Vol 189, © 2019 WIT Press
www.witpress.com, ISSN 1743-3509 (on-line)
doi:10.2495/SAFE190081

Radars have become very common in the automotive fields, as an aid to autonomous driving. These devices exhibit a typical visibility range of 150 m, very high precision and low cost thus making them very suitable for structures monitoring. The detection of vibration of the order of tens of microns can be achieved by software analysis of the phase signals. The very short wavelength of the transmitted signal allows the implementation of the MIMO (Multiple Input Multiple Output) technology, that requires the adoption of arrays of antennas. With MIMO it is possible to implement the Beamforming technology for shaping the radio beam in its form and direction according to the measurements needs. A single radar is then able to monitor multiple targets simultaneously, or different parts of them.

The objective of the present work is to show the applicability of automotive radar to the measurement of oscillations suffered by buildings and bridges, such as to be used as a monitoring tool in the event of earthquakes.

Firstly, a software simulation of an automotive radar is presented, where the reflecting signal is simulated considering an accelerometric acquisition of a real earthquakes. Then a laboratory test is showed, where the vibrating target is simulated using a metallic plane excited by an acoustic transducer, driven by a signal that reproduces traces similar to the ones due to an earthquake. Once the algorithm has been defined and validated, it was carried out an evaluation in a real context. With the aim of analyzing situations similar to those caused by an earthquake, real cases of structures subject to stress are evaluated. As a case of use the oscillation of a viaduct, solicited by heavy traffic, is analyzed.

The paper is organized as follows. After a description of the radar technology considered in Section 2, Section 3 explains the vibrational algorithm, Section 4 introduces the results of the simulations, Section 5 shows the laboratory tests while Section 6 describes the experimental evaluations. Finally, Section 7 concludes the paper.

2 THE FMCW RADAR

In the present paper a radar designed for automotive environment is considered, that operates at the frequency band of 77–81 GHz and implements the Frequency Modulated Continuous Wave (FMCW) technology. This means that the radar is continuously transmitting a signal whose frequency varies periodically. The block scheme for such a kind of radar is depicted in Fig. 1. The upper part of the figure describes the transmission subsystem, while the lower part the reception subsystem. Transmission frequency is generated by the Frequency Generator driven by a Ramp Generator, a block that provides the driver voltage according to the timing of the Timing Generator. At the reception side the received signal is mixed with the transmitted one, providing a signal whose frequency is equal to the difference between the transmitted and the received signals frequencies, being the latter one delayed by the time needed to propagate from the radar to the target, and vice-versa.

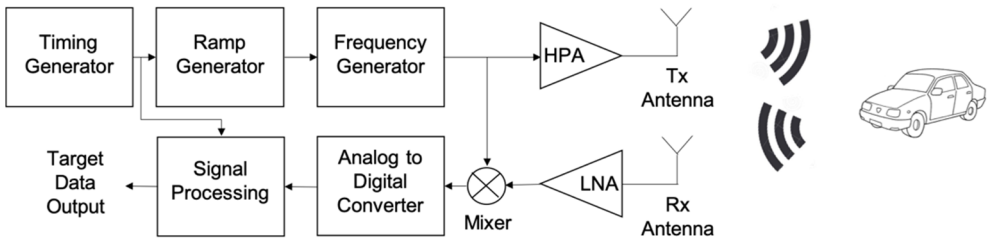

Figure 1: Principle block scheme of an automotive radar.

In FMCW radars the output frequency is linearly modulated from a minimum value f_{start} to a maximum value f_{stop} in the Chirp Time (T_{chirp}) interval, as depicted in Fig. 2; chirp sequences are grouped into frames. From the figure it is possible to note the Idle time, the interval between successive chirps, which can also be zero.

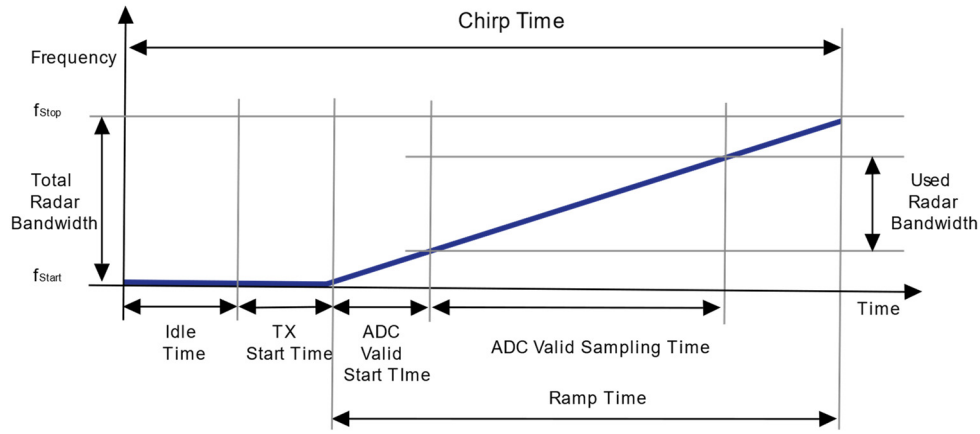

Figure 2: Timing of the Radar Tx frequency.

The output frequency remains constant at the f_{start} value during the Tx start time, needed to switch on the transmitter, while the ADC Valid Start Time defines the starting time for signal sampling, and is introduced with the aim to avoid the first part of the ramp, where the frequency evolution isn't linear. During the ADC Valid Sampling Time the mixed signal is sampled by the ADC; the total number of acquired samples is the ratio between the ADC Valid Sampling Time and the sampling time. Finally, the Ramp End Time ends the frequency transmission. As it is possible to see from the figure, the Used Radar Bandwidth is lower than the Total Radar Bandwidth, being related to the frequency evolution just during the ADC Valid Sampling Time. Radar resolution, the ability to discriminate two nearby objects, is related to the Used Radar Bandwidth and the number of acquired samples. We have to note that a at bigger values of the Used Radar Bandwidth, and then of the number of acquired samples, correspond the radar's ability to discriminate two nearby objects.

For the activity described in the present paper two commercial EVM boards from TI were used, as shown in Fig. 3. The radar board is equipped with the antennas, RF front-end, the mixer, the ADC and a processor that manages the entire board. In the board two Tx antennas and four Rx antennas are present, being each antenna a vertical array of planar antennas. The need of multiple antenna is related to the possibility offered by this board to implement the Multiple Input Multiple Output (MIMO) technology. However, in the considered case the MIMO is not necessary, since the micro-doppler information related to the vibrations that we have to measure can be obtained just from a single receiver. In spite of this, we decided to use a single transmitter ad all four available receivers.

The mixer output provides the beat frequency, which is sampled by the ADCs at a frequency that may be varied from the board configuration panel. The radar board is connected to a FPGA Lattice board through a LVDS BUS; the acquired samples are

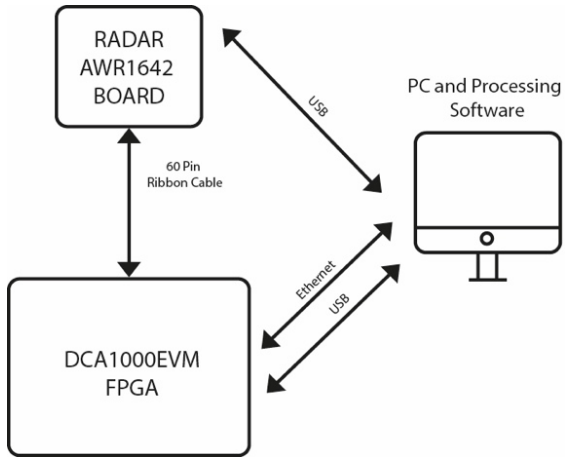

Figure 3: Radar system setup.

reorganized by the FPGA and then sent to a PC for further Matlab processing. The PC manages the configuration of both boards through USB while data are sent through Ethernet. In Table 1 the main details of Radar are reported.

Table 1: Main details of the Radar board.

Frequency	77–81	GHz
Sampling frequency	12	Msps
Maximum bandwidth	4	GHz
Maximum frequency slope	327	MHz/μs
Transmission power	12.5	dBm
Modulation type	FMCW	/
n° Tx–Rx antennas	2–4	/

3 VIBRATION ANALYSIS ALGORITHM AND CONFIGURATION OF THE RADAR

The vibration analysis was based on the work described in [6]. The vibration of the target cannot be identified from the measure of the distance due to the limited spatial resolution R_{def} of the radar, defined by the equation

$$R_{def} = \frac{R_{max}}{n^{o}_{ADC\,samples}/_{2}}. \quad (1)$$

In our case the calibration led to R_{max} of 80 m which, considering the number of samples equal to 4096, provides R_{def} of approximately 4 cm. From this result we see that it is possible to trace oscillations of a target only if the dynamic is at least of 4cm. We have to note that the oscillation of the target produces a sort of modulation on the signal phase due to the variation of the distance radar-target. The oscillation of the target gives rise to a target beat signal equal to:

$$s_{b(t)} = A \exp[j(\omega_b(t) + \emptyset(t))], \quad (2)$$

where $\omega_b(t)$ is the beat frequency due to the mean position of the target and $\emptyset$ (t) is the phase of the signal that is related to its oscillation, equal to

$$\emptyset(t) = \frac{4\pi f_c R_0 + 4\pi f_c x(t)}{c}. \quad (3)$$

The component x(t) is the generic oscillation of the target. The beat signal however does not only contain a component $\omega_b(t)$ of a single target, but also of all echoes detected. In fact, in [6] it is shown that the FFT of $s_b(t)$, fixed $\omega_b(t)$ related to the chosen target, becomes:

$$S_b(f) = \exp(j\emptyset(t)). \quad (4)$$

Referring to Fig. 4, the sampled values of the beat frequency are stored in a matrix, where in the Fast Time are stored the samples related to a chirp time, while in Slow Time are stored data related to the different chirps. In order to evaluate the phase variation of the beat signal in time, a row of the matrix is selected which is related to the distance of the target. The phase variation among the different samples on this row represents the phase change of the beat signal due to the target vibration.

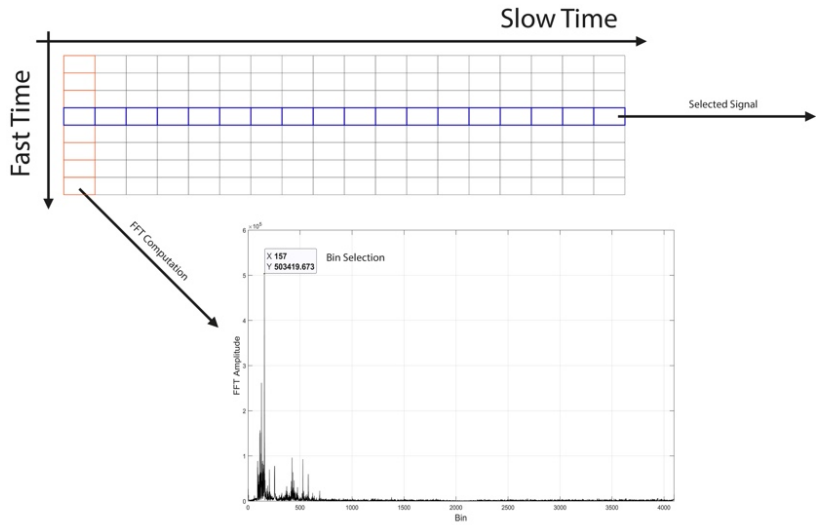

Figure 4: Storage of the beat signal samples.

The steps for extracting the phase information are:

- calculation of the FFT Range for the identification of the Target position;
- identification of the Target and its reference bin (the row on the samples matrix);
- extraction of the FFT phase of the bin;
- representation in time and frequency of the phase signal.

The radar has been configured based on two main parameters, the observation distance and the best resolution. The maximum distance R_{max} is related to the beat frequency f_{beat} through the equation

$$R_{max} = \frac{f_{beat} \cdot c}{2 \cdot p}, \quad (5)$$

where c is the speed of light and p is the slope of the FMCW signal ramp. Given that the maximum value of f_{beat} is equal to the maximum sampling frequency, only the p parameter may be chosen for calibration. The phase signal, used in the analysis, is a signal composed of a value for each chirp and therefore its sampling time coincides with T_{chirp}:

$$f_{Sampling\ FFT} = \frac{1}{T_{chirp}}. \tag{6}$$

This also determines the maximum frequency of observed vibration. The configuration we adopted tries to reduce T_{chirp} to the minimum value and to maximize spatial definition. Based on these constraints, the configuration parameters reported in Table 2 were chosen.

Table 2: Configuration parameters.

Start frequency	77	GHz
Frequency slope	11.587	MHz/μs
Idle time	100	μs
Tx start time	0	μs
ADC valid start time	0	μs
N° ADC samples	4096	/
Sample rate	12	Msps
Ramp end time	345.12	μs
Used radar BW	3998,9	GHz
Frame periodicity	60	ms

The working modulation used is FMCW with upchirp only. As result the maximum detectable distance is 80 m and the maximum detectable oscillation frequency is:

$$f_{Sampling\ FFT} = \frac{1}{T_{chirp}} = \frac{1}{Idle_{Time} + Ramp_{endTime}} = 2.246\ kHz. \tag{7}$$

4 NUMERICAL SIMULATION

In order to verify the ability of the vibration analysis algorithm to extract the evolution in time of a vibration from the radar trace, a Matlab simulation was first performed. In order to represent a realistic trend, the data of a real earthquake, which occurred in Perugia on 30 October 2016, acquired through seismic accelerometers, were taken into consideration [7]. On the basis of the acceleration data, the displacement signal, that is the entity of the vibration, was obtained through a double integration. In simulation, the displacement signal was attributed a maximum amplitude of the order of hundreds of microns, and it was assumed that the analysed target was at a distance of 3 m. The displacement signal R(t) (see Fig. 5) has a number of samples equal to 30,282 with sampling frequency equal to T_{chirp}. The beat frequency is then given by:

$$f_b(t) = 2\frac{R(t) * Ramp_{Slope}}{c}. \tag{8}$$

The value of $f_b(t)$ obtained for each $R(t)$ is used to build a sinusoidal signal $s_b(t)$ that simulates the target:

$$s_b(t) = \exp(-j\,2\,\pi\,f_b(t)\,t). \tag{9}$$

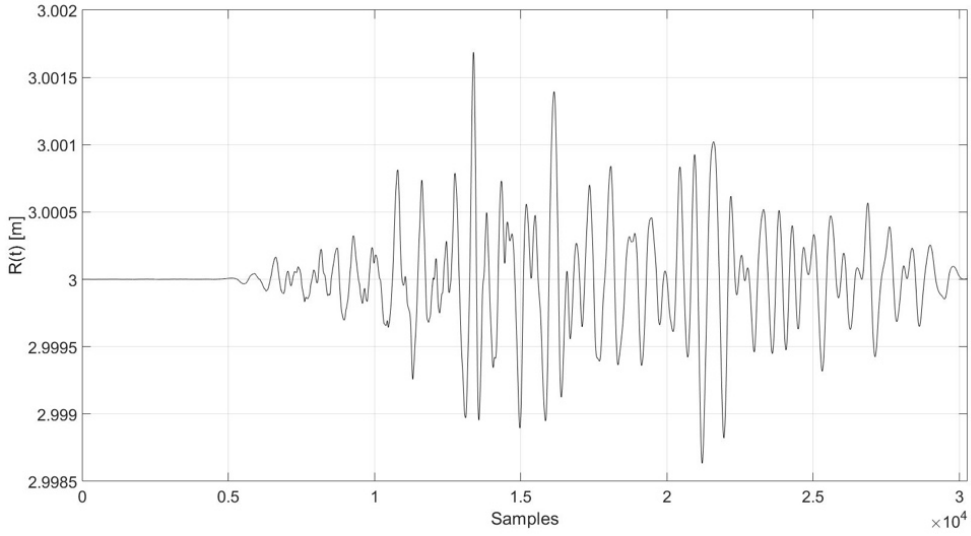

Figure 5: The vibration displacement signal.

Based on this signal, the algorithm was applied, providing the evolution shown in Fig. 6. The almost perfect coincidence of the two evolutions depicted in Fig. 5, the vibration due to the earthquake, and in Fig. 6, the phase extracted from the radar trace following the procedure described above, show the good performance of the vibrational analysis described.

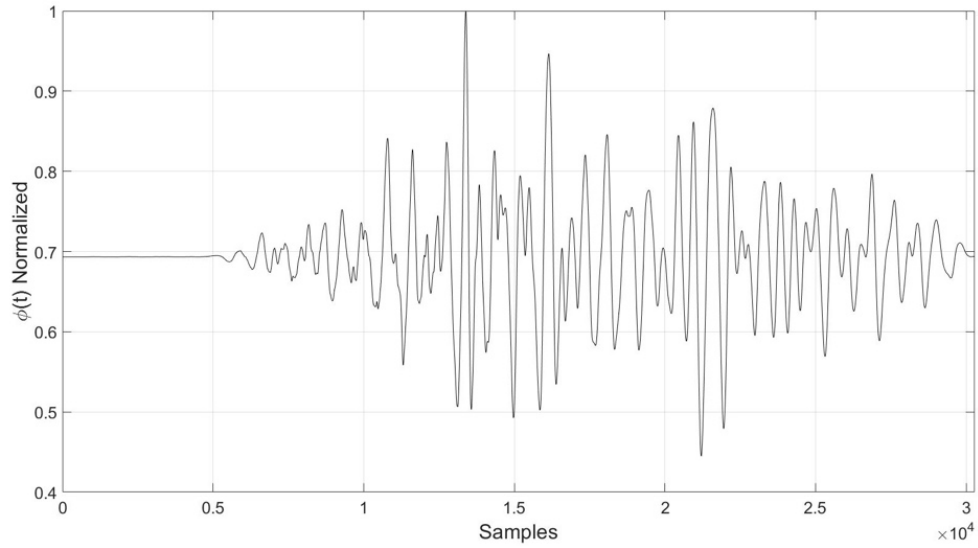

Figure 6: The phase signal provided by the vibrational algorithm.

5 LABORATORY TESTS

To validate the algorithm for vibration measurement it was decided to simulate the oscillation using an electro-acoustic transducer, fixed to a metallic board that simulates the structure under test. To excite the transducer, a train of rectangular pulses with a 50 Hz frequency and a 50% duty cycle was generated. In the measurement setup the board was placed at a known distance of about 2.59 m in order to easily locate its position in the FFT range.

The obtained results are shown in Fig. 7. In the graph of Fig. 7(a) the trend of the phase vs time is depicted, being the acquisition time of about 6 s. In Fig. 7(b) the conversion of the phase into displacement is shown, for a reduced time interval. Finally, the FFT of the displacement signal was obtained to highlight the harmonic vibration components, in order to verify the frequencies triggered by the transducer (see Fig. 7(c)). The most interesting frequency components are at 53.1 Hz and its multiples. In fact the trend of the phase signal over time makes possible to identify a periodicity of about 0.02 s. This is consistent with the type of pulse supplied to the transducer.

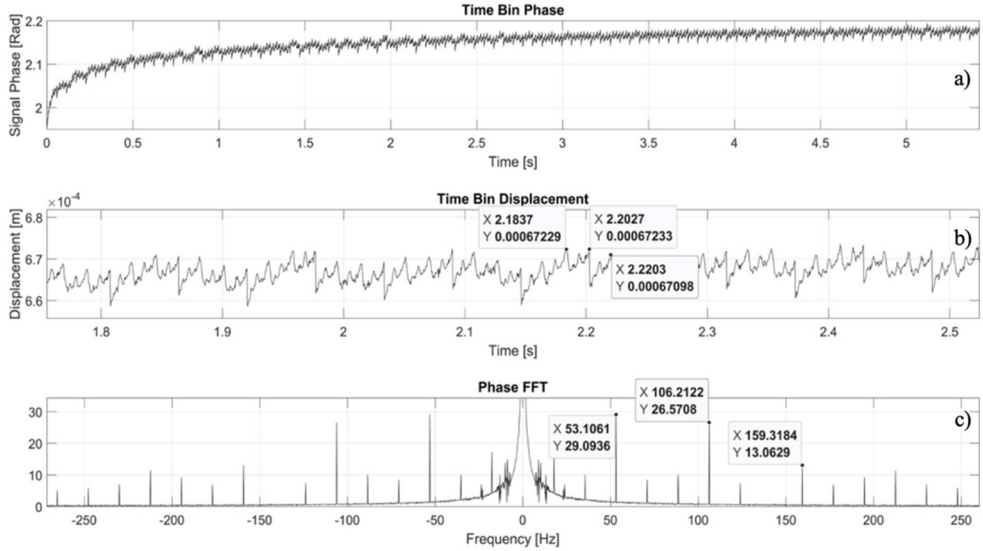

Figure 7: Laboratory test results.

6 EXPERIMENTAL EVALUATION

The last part of the work is aimed at an application in a real context, carrying out measurements on a continuously stressed structure as a motorway bridge. Sensor calibration is the same used in the laboratory environment. Two different tests were performed: in the first one the vibration of the main metal beam of the bridge was measured, while in the second one the vibration of a shelf to support the beam was considered. As introduced in Section 3 the position of the beam and of the shelf were firstly identified in the FFT Range in order to extract from the data matrices the displacement bins.

To validate the obtained results, two videos were recorded showing the passage of the various vehicles on the bridge. There is no perfect synchronization between video and radar acquisitions, but the video is still important for data validation. The results obtained are shown in the Figs 8 and 9. Fig. 8 refers to the radar pointing at the centre of the metal beam

that supports the bridge. The graph shows two important oscillations spaced about 4 s apart. The analysis of the video shows two vehicles that pass on the bridge with a temporal distance of 4 s, causing bridge oscillation. Fig. 9 shows the results obtained with the radar pointing at the steel seismic restrainer of the bridge. Even in this case two important oscillations were found at a distance of about 5 s between them. The analysis of the video shows two trucks crossing the bridge with the same time interval.

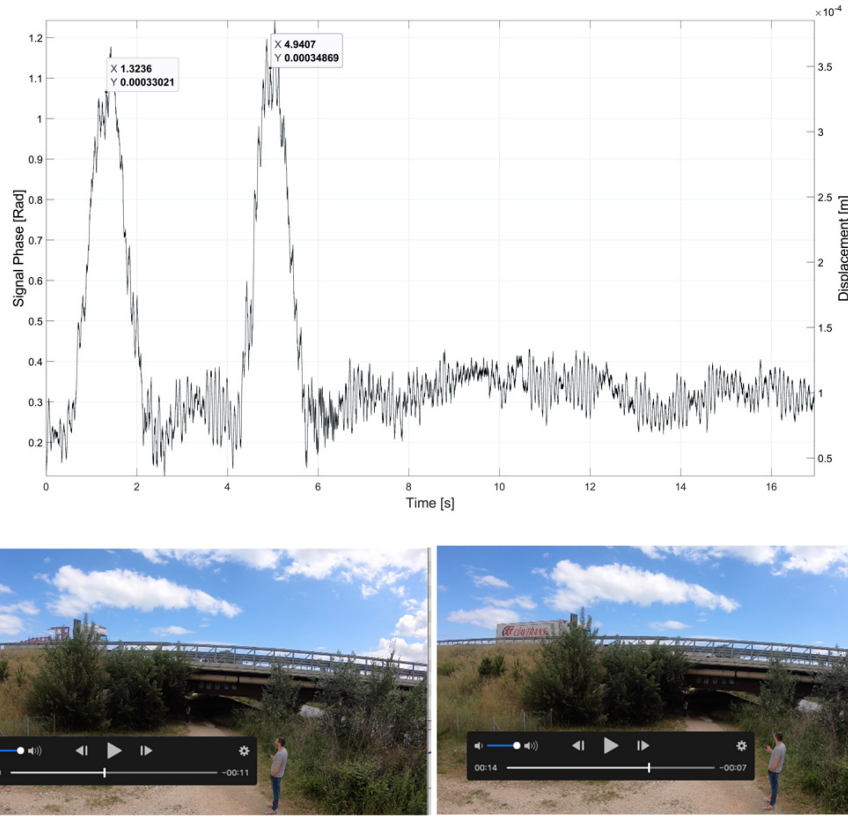

Figure 8: Vibrational test of the main metal beam of the bridge.

7 CONCLUSIONS

In the present paper the adoption of an automotive radar for the evaluation of structural vibration, as the one due to earthquake, was considered. This kind of radar is very promising for a wide range of applications, being characterized by a low cost and good performance. Thanks to its very high operational frequency, the radar and antenna dimensions are reduced, and the corresponding low value of the wavelength allows the analysis of sub-millimetre vibrations through phase analysis algorithms.

The radar performance was tested with numerical simulations, laboratory tests and experimental evaluations. In all the cases the performance was of interest, being the radar able to evidence weak vibrations too. The obtained results demonstrated that such a kind of device, developed for the automotive market, may be applied in different environment with very good performance.

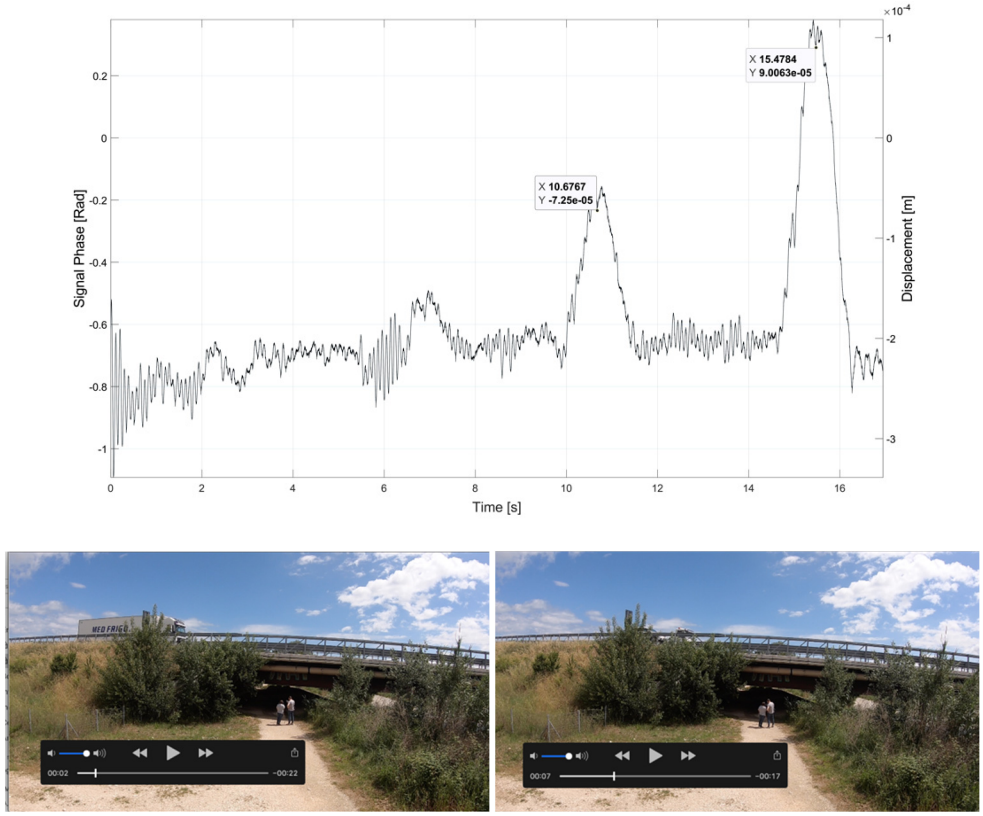

Figure 9: Vibrational test of a steel seismic restrainer of the bridge.

REFERENCES

[1] Concetti, R. et al., IoT solution based on MQTT protocol for real-time building monitoring. *Proceedings of IEEE 23rd International Symposium on Consumer Technologies (ISCT)*, 2019.

[2] Coppi, F., Gentile, C. & Ricci, P.P., A software tool for processing the displacement time series extracted from raw radar data. *AIP Conference Proceedings 1253,* pp. 190–201, 2010.

[3] Luzi, G., Crosetto, M. & Fernandez, E., Radar interferometry for monitoring the vibration characteristics of buildings and civil structures: Recent case studies in Spain. *Sensors (Switzerland)*, **17**(4), p. 669, 2017.

[4] Mei, H., Li, Y., Tian, W. & Zen, T., Weak vibration measurement based on MIMO imaging radar system. *Proceedings of the China International SAR Symposium, CISS 2018*, 2018.

[5] Negulescu, C. et al., Comparison of seismometer and radar measurements for the modal identification of civil engineering structures. *Engineering Structures*, **51**, pp. 10–22, 2013.

[6] Ding, L., Ali, M., Patole, S. & Dabak, A., Vibration parameter estimation using FMCW radar. *Proceedings of the ICASSP, IEEE International Conference on Acoustics, Speech and Signal Processing*, pp. 2224–2228, 2016.

[7] Pierleoni, P. et al., Performance evaluation of a low-cost sensing unit for seismic applications: Field testing during seismic events of 2016–2017 in central Italy. *IEEE Sensors Journal*, **18**(16), pp. 6644–6659, 2018.